A novel enrofloxacin-degrading fungus, Humicola sp. KC0924g, isolated from the rhizosphere sediment of the submerged macrophyte Vallisneria spiralis L.

Xueting Chen

cxtsnow@126.com

Shanghai Fisheries Research Institute, Shanghai Fisheries Technical Extension Station

Yuping Zhang

Shanghai Fisheries Research Institute, Shanghai Fisheries Technical Extension Station

Jinghua Liu

Shanghai Fisheries Research Institute, Shanghai Fisheries Technical Extension Station

Research Article

Keywords: Enrofloxacin, Biodegradation, Humicola sp., Degradation pathway, Comparative transcriptome analysis

Posted Date: October 10th, 2023

DOI: https://doi.org/10.21203/rs.3.rs-3404764/v1

Additional Declarations: No competing interests reported.

Version of Record: A version of this preprint was published at International Microbiology on March 20th, 2024. See the published version at https://doi.org/10.1007/s10123-024-00513-x.

Abstract

Herein, a novel enrofloxacin-degrading fungus was isolated from a rhizosphere sediment of the submerged macrophyte *Vallisneria spiralis* L.. The isolate, designated KC0924g, was identified as a member of the genus *Humicola* based on morphological characteristics and tandem conserved sequences analysis. The optimal temperature and pH for enrofloxacin degradation by strain KC0924g was 28°C and 9.0, respectively. Under such condition, 98.2% of enrofloxacin with initial concentration being 1 mg L^{-1} was degraded after 72 h of incubation, with nine possible degradation products identified. Accordingly, four different metabolic pathways were proposed, which were initiated by cleavage of the piperazine moiety, hydroxylation of the aromatic ring, oxidative decarboxylation, or defluorination. In addition to enrofloxacin, strain KC0924g also degraded other fluoroquinolone antibiotics (ciprofloxacin, norfloxacin, and ofloxacin), malachite green (an illegal addition in aquaculture) and leucomalachite green. Pretreatment of cells of strain KC0924g with Cu^{2+} accelerated ENR degradation. Moreover, it was speculated that one flavin-dependent monooxygenase and/or one laccase involved in ENR degradation based on the increased transcriptional levels of these two genes after Cu^{2+} induction. This work enriches strain resources for enrofloxacin remediation and, more importantly, would facilitate studies on the molecular mechanism of ENR degradation with degradation-related transcriptome available.

Introduction

The output of aquatic products in China ranks at the top worldwide, mainly depending on intensive aquaculture(Han et al. 2020). This type of aquaculture has led to growing problems with microbial diseases, which now require the intensive use of antibiotics. Enrofloxacin (ENR), one type of fluoroquinolone antibiotic (FQs), has been widely used as the feed additive for disease prevention and growth promotion in aquaculture (Ma et al. 2019). However, up to 70% of the ENR was excreted in an unaltered form due to the limitation of absorption and metabolism by aquatic animals, which leads to the frequent detection of residual ENR in the environment (Van Doorslaer et al. 2014). For example, the detection frequency of ENR in samples from Qingshitan Reservoir (South China) was 100%, with the concentrations of ENR ranging from 4.59–6.06 ng L^{-1} (in water), 4.70-331.82 μg kg^{-1} (in sediment) and 6.73-102.87 μg kg^{-1} (in fish muscles). ENR residues have adverse effects on ecosystem functions and introduced the risk of spreadingantibiotic-resistant pathogens, therefore raising public concerns (Riaz et al. 2018, Bhatt and Chatterjee 2022). Thus, removing this antibiotic from the environment is urgently needed.

Physical, chemical and bioremediation methods have been adopted to remove ENR from the environment (Bhatt and Chatterjee 2022). These include adsorption by special materials, photolysis, redox reactions, electrochemical methods, phytoremediation and microbial degradation (Zhang and Huang 2007, Li et al. 2011, Moreira et al. 2020). Among them, bioremediation, such as phytoremediation and microbial degradation, is considered the most promising method due to the economic advantages, high efficiency, no secondary pollution and wide applicability. Phytoremediation is a process that uses a variety of plants

and their associated rhizosphere microbes to degrade, extract, control or immobilize pollutants in the environment(Hoang et al. 2013). Currently, the use of terrestrial and aquatic plants (e.g., *Glycine max* L., *Lactuca sativa* L., *Hordeum vulgare* L., *Cucumis sativa* L., *Acrostichum aureum* L., *Rhizophora apiculata* B1. and *Vallisneria spiralis* L.) for FQs removal has been reported (Boonsaner and Hawker 2010, Ashiq et al. 2021, Abd El-Monaem et al. 2022). In accordance with previous studies, planting submerged plants (*Vallisneria spiralis* L.) for *in situ* remediation of ENR-contaminated sediment originated from aquaculture ponds has been proven feasible by our team (Zhang et al., 2019), with ENR removal efficiencies ranges from 32.3–74.7%. Furthermore, it was referred that ENR removal occurred via plant absorption, photodegradation and biodegradation by rhizosphere microorganisms(Zhang et al. 2019). Further research is needed to better understand the removal mechanism of ENR in sediments to better optimize this bioremediation strategy. Microorganisms are considered to be the most suitable entities for bioremediation because of their physiological abilities and metabolic capacities to degrade or detoxify pollutants. It was evidenced that the brown rot fungus *Gleophyllum striatum* was shown to degrade ENR via extracellular Fenton-type reaction (Wetzstein et al. 1997, Karl et al. 2006). Meanwhile, it was reported that microbial communities in the root sediments of estuarine plants can degrade ENR (Alexandrino et al. 2017, Santos et al. 2019). However, there are very few reports on ENR-degrading pure cultures isolated from the rhizosphere of aquatic plants. As such, isolation and characterization of ENR-degrading strains from this niche could provide strain resources for better application of phytoremediation (e.g., bioaugmentation in the rhizosphere). In addition, it can also provide some clues for a better understanding of the remediation mechanism. The development of microbial genomics or transcriptomics technologies provides new insight into the current understanding of xenobiotic degradation and may lead to new strategies for improving antibiotic degradation (Zhang et al. 2023). For FQs biodegradation, most previous studies have attempted to reveal the mechanisms of biodegradation in the absence of genomic or transcriptomic information.

The aims of this study were three-fold: (1) to isolate an ENR degrader from the rhizosphere sediment of *Vallisneria spiralis* L. which was already proved to mediate ENR remendiation, (2) to investigate the degradation performance of this strain, such as degradation efficiency, key intermediates identification together with intermediates-related residual antibacterial activities, and (3) to initiate as well as advance our understanding of ENR degradation at genetic level with potential catabolic genes revealed via analysis of comparative transcriptome data.

Materials and Methods

Chemicals and media

Enrofloxacin (ENR, 98%), ciprofloxacin (CIP, ≥ 98%), norfloxacin (NOR, 98%), and ofloxacin (OFL, 98%) were purchased from Aladdin Industrial Corporation. Malachite green (MG, 98%) and leucomalachite green (LMG, 98%) were purchased from Sinopharm Chemical Reagent Co., Ltd. Chromatographic grade acetonitrile was purchased from Sigma-Aldrich (St. Louis, USA). All the other chemicals and solvents

obtained from Sinopharm Chemical Reagent Co. Ltd. (China) were of analytical grade. Molecular biology reagents were purchased from Nanjing Nazyme Biotech Co., Ltd. (China).

Mineral salt medium (MM) contained 1.0 g L^{-1} NH_4NO_3, 1.5 g L^{-1} K_2HPO_4, 0.5 g L^{-1} KH_2PO_4, 1.0 g L^{-1} NaCl and 0.2 g L^{-1} $MgSO_4$ (pH 7.0 ~ 7.2). Potato-dextrose (PD) media comprised 5.0 g L^{-1} potato extract power and 20.0 g L^{-1} dextrose. Agar (20.0 g L^{-1}) was added to the PD medium to make solid media plates (PDA). Oat agar (OA), cornmeal agar (CMA), malt extract agar (MEA), and potato carrot agar (PCA) were used for colony morphology examination and were prepared as described previously (Crous 2009). The lysogeny broth plate (LB) used for the residual antibacterial activity assay contained tryptone (10.0 g/L), yeast extract (5.0 g/L), NaCl (10.0 g/L), and agar (20.0 g L^{-1}) at pH 7.0.

Strain isolation and identification

Rhizosphere sediment samples from *Vallisneria spiralis* L. were collected after our previous phytoremediation experiment (Zhang et al. 2019). Thereafter, 5 grams of the sample were added to a 250 mL Erlenmeyer flask containing 100 mL MM with 1 mg L^{-1} ENR. The flask was then placed on a rotary shaker operating at 160 rpm and incubated in complete darkness at 28°C for a period of 7 days. Following enrichment, 5 mL of supernatant from the culture was added to 100 mL of fresh MM with ENR at equivalent concentration. After three consecutive rounds of enrichment, the enrichment solution was then spread on MM agar plates, containing 1 mg L^{-1} ENR, via gradient dilution. Colonies were picked and purified, before evaluated for their ENR-degrading capability.

Colony morphologies were examined on five types of media: PDA, OA, CMA, MEA, and PCA. Cultures were inoculated in a three-point fashion and incubated in the dark at 25°C for 7 days. Colony diameters were measured, and the colors were described according to mycological color charts (RW 1970). The micromorphological description was mainly based on cultures grown on PDA. The mycelium and spores underwent staining with lactophenol blue and were subsequently observed through a light microscope (OLYMPUS®) at a magnification of 640× (16 × 40). Further identification was carried out via analysis of tandem conserved sequences. To this end, three conserved sequences, ITS&LSU, *rpb2*, and *tub2*, serving as representatives of the family *Cheatomiaceae*, were amplified using the relevant primer pairs of ITS5/NL4, rpb2-5F2/rpb2AM-7R, and T1/TUB4Rd, respectively (Table S1). The PCR conditions used were identical to those described by Wang et al. (2016). Each amplicon was purified and sequenced. Sequence alignment was carried out in comparison with thirty-eight other similar and homologous sequences (Table S2) retrieved from the European Nucleotide Archive (ENA) or GenBank portal using the ClustalX tool in MEGA 5 Software (Larkin et al. 2007, Tamura et al. 2011). Phylogenetic typing analyses were conducted using the neighbor-joining tree method.

Biodegradation experiments

A suspension of conidia from strain KC0924g was prepared and adjusted to a concentration of approximately 4.5×10^6 conidia mL^{-1}. The conidial suspension was then inoculated at 5‰ (V/V) into a 150 mL flask containing 50 mL of PD medium and incubated at 28°C and 160 rpm until mycelial pellet

formation (approximately 36 h). To assess the influence of Cu^{2+} on ENR degradation by strain KC0924g, a final concentration of 500 μM Cu^{2+} was added to the culture and allowed to incubate for 24 h. Subsequently, the mycelial pellets were collected via centrifugation (6000 rpm, 5 min), washed twice with MM, and then resuspended in 20 mL MM to create resting cells.

For all the biodegradation experiments, unless stated otherwise, the resting cells were inoculated at approximately 2 mg (dry weight) per mL into a 150 mL Erlenmeyer flask that contained 50 mL of MM with 1 mg L^{-1} ENR. The cultures were incubated at 28°C and 160 rpm on a rotary shaker. Specific samples were collected at predetermined times (0 h, 6 h, 12 h, 24 h, 48 h, 72 h, 120 h, and 168 h), and the amount of residual ENR was assessed using high-performance liquid chromatography (HPLC) with fluorescence detection (FLD). To assess the effect of temperature on degradation, cultures were incubated at temperatures of 15, 20, 28, 35, and 40°C. The effect of initial pH on degradation was assessed by adjusting the pH of the medium to 5.0, 6.0, 7.0, 8.0, 9.0, 10.0, and 11.0. Strain KC0924g was inoculated into MM supplemented with 1 mg L^{-1} CIP, NOR, OFL, MG, and LMG to assess its protential for degrading other FQs, MG and LMG. The control was inoculated with resting cells that had been deactivated by heat. All tests were conducted in triplicate on a rotary shaker (160 rpm) and kept in the dark to prevent photodegradation. Sample cultures were centrifuged and filtered through a 0.22 μm membrane filter to remove impurities and biomass and were then stored at 4°C for further analysis.

The degradation rate (Y) of the compounds mentioned above was quantified using the following equations:

$$Y\ (\%) = 100 \times (C_{CK} - C_T)/C_{CK}$$

where C_{CK} refers to the concentration of the compound in the control test, and C_T pertains to the concentration of the compound in the treatment test.

A first-order kinetic model was created to elucidate the degradation efficiency of ENR by strain KC0924g with or without Cu^{2+} treatment.

$$\ln (C_0 / C_t) = kt$$

$$t_{1/2}=\ln 2/k$$

where C_0 and C_t refer to the concentration (mg L^{-1}) of ENR at time zero and time t, respectively; k represents the ENR degradation rate constant (h^{-1}); and $t_{1/2}$ (h) denotes the half-life time for ENR degradation.

Chemical analysis

The FQs concentrations present in the cultures were measured through the use of an Agilent 1260 HPLC system equipped with an Eclipse Plus C_{18} reversed-phase column (250 mm×4.6 mm, 5 μm particle sizes,

Agilent) along with fluorescence detection. This method utilized the retention time and peak area of pure standards, and had an excitation wavelength of 280 nm and emission wavelength 450 nm for ENR, CIP, and NOR, and an excitation wavelength 283 nm and an emission wavelength of 490 nm for OFL. The mobile phase consisted of phosphoric acid-triethylamine (0.05 M, pH 2.4) and acetonitrile (18:82, v/v). The flow rate used was 1.0 mL min^{-1}.

The metabolites were detected using ultra-performance liquid chromatography coupled with a Q Exactive HF-X mass spectrometer (Thermo Fisher Scientific), which was equipped with an electrospray ionization (ESI) probe. The UPLC-HRMS parameters were as follows: the column used was Hypersil GOLD C_{18} column (100 mm × 2.10 mm, particle size: 3 μm, Thermo Fisher Scientific), the flow rate was set at 0.2 ml min^{-1}, and injection volume at 5 μL with mobile phase comprising of solvents A (ultrapure water containing 0.1% v/v formic acid) and B (acetonitrile). Separation was conducted for 30 min under these conditions. 0 ~ 4 minutes: Maitain the volume ratio of solution B at 30%. 4 ~ 21 minutes: Increase the volume of solution B from 30–95%. 21 ~ 25 minutes: Keep the volume of solution B at 95%. 25 ~ 30 minutes: Reduce the volume ratio of solution B back to 30%. The ionization method used was positive ion, and the ion transmission temperature, source voltage, protective gas, and auxiliary gas were 300°C, 4 kV, 35 arb, and 10 arb, respectively. The data analysis software employed was Xcalibur.

Solid-phase extraction combined with high-performance liquid chromatography-tandem mass spectrometry (SPE-HPLC—MS/MS) was used to detect residues of MG and LMG in the cultures. Following the manufacturer's guidelines, MG and LMG were extracted, enriched, and eluted using PRS columns (Thermo Fisher Scientific). The HPLC—MS/MS conditions were as follows: Column: Thermo C18 chromatographic column (100 mm×2.1 mm); The separation process was executed at a flow rate of 0.2 mL/min with an injection volume of 10 μL. The mobile phase was composed of acetonitrile solvents B and 0.2% ammonium acetate solvent D. The process was carried out for 10 mins, with the flow rate at 0.2 mL/min. 0 ~ 1.50 minutes: Increase the volume of solution D from 0 to 35%. 1.50 ~ 1.51 minutes: Decrease the volume of solution D from 35–10%. 1.51 ~ 4.50 minutes: Maintain the volume ratio of solution D at 10%. 4.50 ~ 4.51 minutes: Increase the volume of solution D from 10–35%. 4.51 ~ 9.00 minutes: Maintain the volume ratio of solution D at 35%. 9.00 ~ 10.00 minutes: Reduce the volume ratio of solution D to 0%.

Residual antibacterial activity assay

The antibacterial activity of degradation products of FQs against nonresistant *Escherichia coli* DH5α (Gram-negative) was evaluated using the agar plate diffusion method (punch method). In brief, 500 μL of log-phase *E. coli* DH5α culture was spread on LB plates. Six dispersed wells were then drilled in each plate using a sterile 8 mm diameter punch. Three of the six wells in each plate were injected with the FQs solution and the other three with the corresponding degradation product solution. Each sample was injected into the well in a volume of 200 μL and the plates were incubated in a constant temperature incubator at 37°C for 20 hours. The inhibition circle diameter (Φ) was measured using a digital vernier

caliper. The relative inhibition rate (R) of the degradation product was evaluated by comparing the inhibition zone sizes of the product and drug solutions.

$R\ (\%) = 100 \times (\Phi_p\text{-}8)/(\Phi_m\text{-}8)$

where Φ_p and Φ_m represent the inhibition circle diameter of degraded product and FQs drug, respectively.

Comparative transcriptome analysis

Sample preparation, RNA extraction, cDNA library construction, and Illumina HiSeq sequencing

Mycelial cells with or without Cu^{2+} treatment for comparative transcriptome sequencing were obtained as described in 2.3. The obtained cells were immediately washed three times with sterile PBS buffer and stored at -80°C before further treatment. Each treatment was performed in three independent experiments. Total RNA was extracted from mycelia using TRIzol® reagent according to the manufacturer's instructions (Invitrogen), and genomic DNA was removed using DNase I (TaKaRa). RNA quality was then determined using a 2100 Bioanalyzer (Agilent) and quantified using an ND-2000 (NanoDrop Technologies). High quality RNA samples (OD260/280 = 1.8 ~ 2.2, OD260/230 ≥ 2.0, RIN ≥ 6.5, 28S:18S ≥ 1.0, > 10 μg) were used to construct a sequencing library. The cDNA library was prepared using a TruSeqTM RNA Sample Preparation Kit from Illumina (San Diego, CA) and sequenced using an Illumina NovaSeq 6000 sequencer (150 bp*2, Shanghai BIOZERON Co., Ltd.).

De novo assembly, annotation, and differential expression analysis

Raw paired-end reads were trimmed and quality controlled using Trimmomatic with parameters (http://www.usadellab.org/cms/uploads/supplementary/Trimmomatic). RNA *de novo* assembly was performed using Trinity (http://trinityrnaseq.sourceforge.net/) with clean data from from all samples. All the assembled transcripts were searched against the NCBI Protein Nonredundant (NR), String, and KEGG databases using BLASTX to identify proteins with the highest sequence similarity to the given transcripts and to retrieve their functional annotations. The expression level of each transcript was calculated using the reads per kilobase of exon per million mapped reads (RPKM) method, and differentially expressed genes (DEGs) with a P value < 0.05 and |log2 (fold change)| (|log2FC|) ≥ 2 were selected by comparing the CU and CK groups. Finally, the DEGs were annotated and analyzed in the Gene Ontology (GO) and Kyoto Encyclopedia of Genes and Genomes (KEGG) databases.

Data analysis and nucleotide sequence accession numbers

All experiments were repeated three times, and the data are presented as the mean ± standard deviation. Differences between treatments were analyzed by one-way ANOVA and Duncan's multiple range tests at $P < 0.05$ using IBM SPSS Statistics 26 (IBM Crop., Armonk, NY, USA).

The GenBank accession numbers for the ITS, ITS&LSU, *rpb2*, and *tub2* gene sequences of strain KC0924g were ON055749, ON025176, ON033740, and ON033741, respectively. The raw sequence reads for the transcriptome of strain KC0924g have been submitted to the NCBI Sequence Reads Archive (SRA) database under the SRA accession number: PRJNA1022865.

Results and DiscussionIsolation and identification of the ENR-degrading fungus

A filamentous fungal strain, KC0924g, exhibiting a high ENR degradation ability, was isolated from the rhizosphere sediment sample. Colonies of strain KC0924g on PDA were 47 to 58 mm in diameter after 7 days at 25°C, with entire edges. The aerial mycelium was thick, white to yellow and olivaceous black in reverse (Fig. 1a). The colony morphologies of strain KC0924g grown on four other different media (OA, CMA, MEA, and PCA) are shown in Fig. S1, and their characteristics are described in the figure legend. Strain KC0924g possessed thick-walled conidia and an acremonium-like synanamorph (Fig. 1bc). The above morphological characteristics of strain KC0924g were similar to those of the model strain *Humicola pulvericola* CBS 723.97^{T} (Wang et al. 2019). A BLASTN search against the sequences on the National Center for Biotechnology Information (NCBI) website revealed that the ITS gene sequence of strain KC0924g shared 98.99% similarity to *Humicola* sp. JS-0112 and *Chaetomium* sp. TR160. Hence, the rDNA-ITS sequence alone cannot distinguish the taxonomic status of strain KC0924g. It was found that the 5.8S nrRNA gene region and the D1/D2 domains of the 28S nrDNA (ITS&LSU), the second largest subunit of the DNA-directed RNA polymerase II gene region (*rpb2*) and the partial beta-tubulin gene region (*tub2*) were used as DNA barcodes to differentiate *Humicola* species and related genera in *Chaetomiaceae* (Wang et al. 2016). Subsequently, the phylogenetic tree (Fig. 1d) built based on the ITS&LSU-*rpb2-tub2* gene sequences of strain KC0924g and related strains revealed that strain KC0924g clustered with *Humicola pulvericola* CBS 723.97^{T} (Wang et al. 2019). Combining the morphological characteristics with phylogenetic analysis, the ENR degrader was identified as a member of the genus *Humicola* and deposited at the China Center for Type Culture Collection (deposition number: CCTCC M 2020752).

Fungi of the genus *Humicola* are common and widespread and are known to have biotechnological and industrial potential (Ibrahim et al. 2021). In recent years, the genus *Humicola* has been found to be valuable for environmental remediation. For example, *Humicola* sp. 2 WS1 showed marked arsenic biomethylation potential. Through bioaugmentation, *Humicola* sp. 2 WS1 not only attenuated the stressful effects of arsenic on *Bacopa monnieri* L. in the rhizosphere environment but also promoted the growth of *B. monnieri* (Tripathi et al. 2020). In this study, *Humicola* sp. KC0924g was isolated from the rhizosphere sediment sample of the submerged macrophyte *V. spiralis.* Submerged macrophytes play an essential role in maintaining aquatic ecosystem stability and are widely used in the remediation of contaminated water and sediment (Dai et al. 2014). Further work is required to explore the effect of *Humicola* sp. KC0924g and *V. spiralis* interaction on sediment remediation. Admittedly, this is the first report that a *Humicola* species can degrade the antibiotic ENR.

Degradation of ENR by strain KC0924g

Temperature and pH are two critical environmental factors that impact xenobiotic degradation. This is due to the influence of temperature on the growth of microorganisms and the activity of certain catabolic enzymes, as well as the impact of the initial pH of the medium on the movement of compounds to microorganisms and the alteration in the solubility of contaminants. Therefore, the effects of different temperatures and the initial pH value of the medium on ENR degradation were studied separately. Among five temperatures ranging from 15°C to 40°C, the optimum degradation temperature was observed at 28°C with maximum degradation of 89.6%. When the temperature lowered to 15°C, the rate of degradation decreased to 69.4%. Subsequently, with an increase in the temperature to 40℃, the degradation efficiency surpassed 76.9%. Overall, *Humicola* sp. KC0924g exhibited relatively broad temperature adaptability for ENR degradation. The degradation rate of ENR affected by temperature was listed in the following order: 28℃>20℃≧35℃>40℃>15℃ (Fig. 2a). The optimum temperature for photosynthesis in temperate submerged plants is usually between 25 ~ 32°C (Barko et al. 1982, Santamaría and van Vierssen 1997, Pedersen et al. 2013). As can be seen from the results, the optimal temperature interval for ENR degradation by *Humicola* sp. KC0924g was consistent with that for the growth of temperate submerged plants. Subsequently, the effect of different pH values (ranging from 5.0 to 11.0) on the degradation of ENR by *Humicola* sp. KC0924g was investigated at the optimum temperature of 28°C. The degradation rate was not significantly different when the initial pH was 7.0, 8.0 and 9.0 ($p>0.05$), and the maximum degradation rate was as high as 98.2% at pH of 9.0. The degradation rate decreased significantly when the initial pH was below 6.0 or above 10.0. The degradation extents of ENR affected by pH were ranked in the following order: pH9.0 ≥ pH8.0 ≥ pH 7.0>pH 10.0>pH 6.0 (Fig. 2b). The above experiments showed that this strain could degrade ENR efficiently under neutral to slightly alkaline conditions. The optimal pH range required for fish and shrimp growth in aquaculture is between 7.5 and 8.0 (Liu and Wang 2012). During this range, ENR can be efficiently degraded by strain KC0924g. The dynamic degradation curve of ENR (initial concentration of 1 mg L^{-1}) under the optimal condition (28°C and pH 7.0) by strain KC0924g is shown in Fig. 2c. The degradation rate increased immediately during the first 12 h, then gradually slowed down between 12 h and 72 h and remained stable after 72 hours.

Identification of the metabolites and proposed ENR degradation pathways

Nine metabolites were preliminarily detected in the catabolic supernatant by means of ultra-performance liquid chromatography coupled with high-resolution electrospray ionization mass spectrometry (UPLC-HRMS) (shown in Fig. 3). All identified peaks were found to correspond to protonated derivatives of the theoretical values of the corresponding compounds with errors between − 1.39 and 0.04 ppm (shown in Table 1). In contrast, no corresponding mass spectrum peaks of these metabolites were found in the control. Four metabolic pathways were proposed based on the identified metabolites (Fig. 4). In Pathway

I, ENR underwent transformation through the splitting of the piperazine moiety, resulting in the production of Compounds C1 and C2. According to Adjei et al. (2006), it was believed that the antibacterial activities of Compounds C1 and C2 were reduced due to the cracking of the piperazine ring. In Pathways II, III, and IV, ENR underwent biotransformation through hydroxylation of the aromatic core, oxidative decarboxylation, and oxidative defluorination to generate C3, C4, and C5, respectively. For C5, further pathways existed. These included pathway iv1 and pathway iv2. In pathway iv1, C6 was created by further hydroxylation of C5 at the aromatic core. In pathway iv2, C7 was produced by oxidative removal of the cyclopropyl group from the quinoline ring of C6. Afterward, the piperazine ring of C7 slowly degraded through C-N bond cleavage, yielding C8 and C9.

Table 1
Spectral data for ENR and postulated biodegradation metabolites determined from UPLC-HRMS

Compound	Peak mass $[M+H]^+$ (*m/z*)	Display Formula	Theo. mass $[M+H]^+$ (*m/z*)	Delta (ppm)*	RT (min)	References
ENR	360.1713	$C_{19}H_{23}O_3N_3F$	360.17180	-1.39	11.25	
C1	334.1559	$C_{17}H_{21}O_3N_3F$	334.15615	-0.88	3.99	(Wetzstein et al. 1997, Karl et al. 2006)
C2	263.0826	$C_{13}H_{12}O_3N_2F$	263.08265	-0.14	1.81	
C3	376.1663	$C_{19}H_{23}O_4N_3F$	376.16671	-1.20	1.21	
C4	332.1768	$C_{18}H_{23}O_2N_3F$	332.17688	-0.19	1.11	
C5	358.1761	$C_{19}H_{24}O_4N_3$	358.17613	0.04	3.69	
C6	374.1708	$C_{19}H_{24}O_5N_3$	374.17105	-0.64	0.83	
C7	318.1446	$C_{16}H_{20}O_4N_3$	318.14483	-0.66	3.10	This study
C8	249.0870	$C_{12}H_{13}O_4N_2$	249.08698	-0.09	12.41	This study
C9	235.0713	$C_{11}H_{11}O_4N_2$	235.07133	-0.25	10.91	This study

*Generally, a mass error between − 5 ppm and 5 ppm is acceptable (Blake et al. 2011).

Previous studies have shown that basidiomycetes fungi decay wood and degrade certain xenobiotics due to their ability to produce hydroxyl radicals (H_2O_2), which trigger an extracellular Fenton-type reaction(Jensen et al. 2001). A total of 137 ENR metabolites produced by *Gloeophyllum striatum* and other basidiomycetous fungi were identified, in which the principal routes for ENR metabolism include hydroxylation of the aromatic core, oxidative decarboxylation or defluorination, or decomposition of the piperazine moiety and N-oxidation (Wetzstein et al. 1997, Karl et al. 2006, Wetzstein et al. 2006, Parshikov and Sutherland 2012). In this study, ENR major metabolites catalyzed by the ascomycete fungi *Humicola*

sp. KC0924g were similar but differed slightly from those of *Gloeophyllum striatum*. The presence of the fluorine atom at the R6 position, the piperazine ring at the R7 position, and the cyclopropyl group at the R1 position in FQs improves the antibacterial effect of the drug and reduces the compatibility of the drug with microbial degradation (Van Caekenberghe and Pattyn 1984, Bhatt and Chatterjee 2022). In Pathway IV to iv2, ENR first underwent hydroxyl substitution to remove the fluorine group, then the cyclopropyl group was removed, and finally, the piperazine ring gradually cracks. As the three essential functional groups in the ENR molecule were consecutively degraded, we speculated that this pathway might diminish the antibacterial efficacy of ENR while enhancing its degradability. However, due to the low concentration of the metabolites, the information obtained from UPLC-HRMS alone is not sufficient to fully analyze their chemical structures. The exact stereochemistry of these trace metabolites will be determined in future work by enriching and purifying the metabolites followed by NMR spectroscopy.

Degradation of other fluoroquinolones, malachite green, and leucomalachite green by strain KC0924g

Strain KC0924g showed degradative capabilities against additional types of FQs, such as including CIP, NOR, and OFL. The removal rates of CIP, NOR, and OFL by strain KC0924g after 72 h of incubation were 86.4%, 70.2%, and 46.4%, respectively (Fig. 2d). It was found that the different types of FQs have similar molecular configurations and follow similar biodegradation pathways, but slight differences in their molecular structures or different toxicities to microorganisms could lead to altered degradation rates (Parshikov and Sutherland 2012, Bhatt and Chatterjee 2022). FQs have similar chemical structures but different toxicities to microorganisms, which may explain why KC0924g is able to degrade different classes of FQs at different rates.

Furthermore, strain KC0924g could also degrade MG and LMG (Fig. 2d and Fig. S2). The degradation rate of MG reached 99.9% without accumulating LMG and that of LMG reached 87.5%. MG is a synthetic triphenylmethane dye with strong bactericidal, fungicidal and parasiticidal properties (Srivastava et al. 2004). As a result, MG was once extensively applied in fisheries to prevent and control diseases, such as saprolegniasis, white spot disease, and ciliate disease (Bergwerff and Scherpenisse 2003, Srivastava et al. 2004). LMG is the major reductive metabolite of MG, which persists in fish tissues and the environment for long periods of time (Li et al. 2012). The use of MG in aquaculture is now strictly prohibited as MG and LMG have been shown to be toxic and carcinogenic (Lin et al. 2016). However, residues of MG and LMG are often detected in the aquaculture environment. Therefore, MG must be removed from the environment to prevent potential harm to human health. The ability of strain KC0924g to degrade many common contaminants in the aquaculture environment makes it a good candidate for environmental remediation.

Residual antibacterial activity assay

The antibacterial activity of the supernatants against the gram-negative bacterium *E. coli* DH5α (non-resistant) was measured directly by means of the agar diffusion method. The residual antibacterial activity was expressed as a percentage of the initial drug (1 mg L^{-1}). After 72 hours of degradation by strain KC0924g, the antibacterial activities of the four FQs (ENR, CIP, NOR and OFL) in the supernatants decreased by approximately half, with residual antibacterial activities of 51.57%, 56.63%, 37.73% and 44.72%, respectively (shown in Fig. 5). In addition, a control with the supernatant of strain KC0924g after 72 h incubation in MM medium (without FQs) showed no antibacterial activity against *E. coli* DH5α, ruling out the effect of endogenous fungal antimicrobials in this experiment. Parent drugs that have not been completely degraded and degradation products with antimicrobial groups (e.g. piperazine groups) may account for the residual antibacterial activity in the supernatants. Čvančarová et al. (2015) showed that the supernatant of FQs degraded by ligninolytic fungi still exhibited high residual antibacterial activity against gram-negative and gram-positive strains that were not resistant to FQs in the environment. Wetzstein et al. found that the residual antibacterial activity of CIP supernatant against gram-negative *Escherichia coli* ATCC 8739 was attenuated after 13 weeks of degradation by species of basidiomycetes (Wetzstein et al. 1999). After degradation by a *Thermous* sp. isolate, the residual antibacterial activity of the supernatant of four FQs against *Escherichia coli* K12 decreased by 20–40% (Pan et al. 2018).

Cu^{2+} treatment increased the efficiency of ENR removal by strain KC0924g

It was observed that resting cells of strain KC0924g treated with Cu^{2+} displayed a higher efficiency of ENR removal in comparison to untreated resting cells. The removal of ENR by cells of strain KC0924g with or without Cu^{2+} treatment could be fitted by the first-order kinetic model. Table 2 presents the values for k (0.0308, 0.0763) and R^2 (0.931, 0.969), demonstrating that the first-order kinetic model corresponds to the data well. The half-life of ENR (1 mg L^{-1}) measured in Cu^{2+}-treated cells reached 3.9 h, compared to 9.8 h obtained in untreated cells. Moreover, the removal rate of ENR in Cu^{2+}-treated cells within 24 h reached 98.9%, a higher value than the 77.39% measured in untreated cells. The negligible change in ENR concentration upon treatment with Cu^{2+} alone (in the absence of microorganisms) confirmed that microorganisms dominate ENR degradation. The results showed that the addition of Cu^{2+} could greatly improve the degradation efficiency of ENR by strain KC0924g. This study is consistent with some previous studies indicating that low levels of Cu^{2+} may promote xenobiotic degradation. For example, Xu and Wang (2014) found that low concentrations of Cu^{2+} stimulated the degradation efficiency of decabromodiphenyl ether by the white rot fungus *Phlebia lindtneri* JN45(Xu and Wang 2014). Similarly, Sangare et al. (2014) demonstrated that Cu^{2+} is an activator of aflatoxin B1 degradation by *Pseudomonas aeruginosa* N17-1(Sangare et al. 2014).

Table 2
Kinetic parameters and removal of ENR (1 mg L^{-1}) by strain KC0924g (induced by Cu^{2+}) after a 24 h incubation

Cu^{2+} (μM)	k (h^{-1})	$T_{1/2}$ (h)	R^2	Removal (%)
0	0.0308	9.8	0.931	77.39
500	0.0763	3.9	0.969	98.94
k-Kinetic removal rate constant (h^{-1});				
$T_{1/2}$-Degradation half-life (h);				

R^2-correlation coefficient.

Comparative transcriptome analysis of strain KC0924g with and without Cu^{2+} treatment

Six libraries were constructed from mRNA of control (CK) and Cu^{2+}-treated (CU) samples to investigate the transcriptomic responses to Cu^{2+} in strain KC0924g. These libraries each generated approximately 53 million, 74 million, 53 million, 53 million, 57 million and 51 million raw reads, and after quality control, over 88% and 83% of clean reads were obtained from CK samples (CK-1, CK-2 and CK-3) and Cu^{2+}-treated samples (CU-1, CU-2 and CU-3), respectively (Table S3). After de novo assembly using Trinity software, 24531 unigenes were obtained, with an average length of 1513 bp and an N50 of 2519 bp. The number and percentage of unigenes with significant similarity to sequences in the NR, GO, COG, KEGG and SWISS-prot databases are listed in Table S4. Generally, 21,527 unigenes were annotated in at least one database, accounting for 87.75%. Comparative transcriptome analysis was performed to explore the differentially expressed genes (DEGs) between the CK and CU groups. A total of 11570 genes were identified as DEGs in one group relative to the other group. In the CU group, 275 genes were upregulated and 11,295 genes were downregulated compared to the CK group (Fig. 6a, b), indicating that Cu^{2+} has a repressive impact on the expression of the majority of DEGs. Gene Ontology (GO) enrichment analysis was conducted to identify the primary functional categories of DEGs. As shown in Fig. 6c and Table S5, the DEGs were mainly enriched in the GO categories of biological processes (BP) and cellular component (CC). The top three enriched items were plastid (genes number = 1509, cellular component category, GO:0009536), chloroplast (genes number = 1481, cellular component category, GO:0009507) and developmental process (genes number = 1361, biological processes category, GO:0032502). The Kyoto Encyclopedia of Genes and Genomes (KEGG) enrichment analysis of the DEGs identified 37 significantly enriched pathways ($P<0.05$), of which ribosome (ko03010), carbon metabolism (ko01200) and protein processing in the endoplasmic reticulum (ko04141) were the top three enriched pathways (Fig. 6d and Table S6).

Most of the detected DEGs involved in xenobiotic biodegradation and metabolism were downregulated. However, only two genes encoding FAD-dependent monooxygenase (TRINITY_DN2180_c0_g1:K00480) and a hypothetical protein (TRINITY_DN13314_c0_g1) were found to be upregulated (Table S7). FAD-dependent monooxygenase (FMO), an oxidoreductase with flavin adenine dinucleotide or flavin mononucleotide as a coenzyme, is involved in diverse biochemical redox reactions and the synthesis of intricate natural products (van Berkel et al. 2006, Huijbers et al. 2014). In nature processes, FMO catalytic activity initiates the breakdown of xenobiotics, and bacteria have also used this catalytic activity to degrade or inactivate clinically used antibiotics(Reis et al. 2021). A class A FMO, bacterial tetracycline destructase (TetX), has been discovered to hydroxylate the C11a of tigecycline, causing it to become inactivated by producing 11a-hydroxytigecycline (Volkers et al. 2011). Rifampicin monooxygenase (Rox) is another class A FMO that was propsed to catalyze the hydroxylation of C2 in rifampicin, resulting in the generation of 2'-N-hydroxy-4-oxo-rifampicin based on an NMR analysis of the Rox crystal structure(Hoshino et al. 2010). On the other hand, BVMO (Baeyer-Villiger monooxygenase) is a class B FMO that has been discovered to oxidize the carbonyl moiety of the β-lactam ring (Minerdi et al. 2016). Molecular docking studies have identified active sites within the crystal structure that interact with vancomycin and/or methicillin (Hwang et al. 2018). Furthermore, the sulfonamide monooxygenase (SadA/SadC) constitutes a two-component FMO system that facilitates the conversion of sulfamethoxazole to products that lack antimicrobial activity (Ricken and Kolvenbach 2017). The upregulated FMO (TRINITY_DN2180_c0_g1) in this research probably accommodates the ENR for oxidative reactions. Nonetheless, further investigation is necessary to unravel the precise role of this FMO.

A previous report indicated that laccase and cytochrome P450 enzymes play roles in FQs degradation by white-rot fungi (Prieto et al. 2011, Gao et al. 2018). Through transcriptome analysis, we found that only one laccase gene (TRINITY_DN6638_c0_g1) was upregulated in the CU group, and no significantly upregulated genes encoding cytochrome P450 enzymes were found in the same group. The BLAST results indicated that the amino acid sequence similarity of this particular sequence with the laccase sequences from *Trametes versicolor* and *Phanerochaete chrysosporium* were 24.26% and 25.99%, respectively (Fig. 7). For comparison, the amino acid sequence similarity of the laccases from *Trametes versicolor* and *Phanerochaete chrysosporium* was 26.91%, and both laccases have been previously observed to biotransform FQs. The laccase activity of strain KC0924g was not detected, possibly due to low quantity and activity of extracellular laccase. Futher attempts to increase the laccase concentration will be made to study its catalytic function. The transcriptome analysis of strain KC0924g highlighted potential biodegradation-related enzymes, which could assist in future investigation of the microbial degradation molecular mechanism of FQs.

Conclusions

Humicola sp. KC0924g was isolated for its ability to degrade ENR from rhizosphere sediments from a previous phytoremediation experiment. The optimum conditions for ENR degradation by strain KC0924g were at 28°C and pH of 9.0. The biodegradation metabolites were detected and identified using UPLC-HRMS, and four distinct pathways were proposed. Additionally, strain KC0924g demonstrated the ability

to decompose MG, LMG and three other types of FQs. The degradation efficiency of ENR by strain KC0924g can be significantly improved by Cu^{2+}. An FMO and a laccase were predicted to be involved in the degradation process of ENR based on comparative transcriptomic analyses. The successful isolation of strain KC0924g offers a potential candidate strain for bioremediation applications and an opportunity for further investigation into the interactions between fungi and plants in the rhizosphere, as well as subsequent clues to the molecular mechanisms of ENR degradation.

Declarations

Ethics approval and consent to participate: Not applicable.

Consent for publication: All authors have read the manuscript and agreed to its publication.

Availability of data and material: Not applicable.

Competing interests: The authors declare no conflicts of interest.

Funding: This research was supported by the Shanghai Agriculture Applied Technology Development Program, China (Grant No. 2020-02-08-00-07-F01483), the National Natural Science Foundation of China (31900097), and the Natural Science Foundation of Shanghai (20ZR1450800).

Authors' contributions: Xueting Chen and Yuping Zhang conceived and designed the experiments; Xueting Chen and Jinghua Liu performed the experiments and analyzed the data; Xueting Chen wrote and submitted the paper. All authors have read and agreed to the published version of the manuscript.

Acknowledgements: This research was supported by the Shanghai Agriculture Applied Technology Development Program, China (Grant No. 2020-02-08-00-07-F01483), the National Natural Science Foundation of China (31900097), and the Natural Science Foundation of Shanghai (20ZR1450800).

References

1. Abd El-Monaem, E. M., A. S. Eltaweil, H. M. Elshishini, M. Hosny, M. M. Abou Alsoaud, N. F. Attia, G. M. El-Subruiti and A. M. Omer (2022) Sustainable adsorptive removal of antibiotic residues by chitosan composites: An insight into current developments and future recommendations. Arabian Journal of Chemistry 15(5):103743. https://doi.org/10.1016/j.arabjc.2022.103743
2. Adjei, M. D., T. M. Heinze, J. Deck, J. P. Freeman, A. J. Williams and J. B. Sutherland (2006) Transformation of the antibacterial agent norfloxacin by environmental mycobacteria. Applied and environmental microbiology 72(9):5790-5793. 10.1128/aem.03032-05
3. Alexandrino, D. A. M., A. P. Mucha, C. M. R. Almeida, W. Gao, Z. Jia and M. F. Carvalho (2017) Biodegradation of the veterinary antibiotics enrofloxacin and ceftiofur and associated microbial community dynamics. Science of the Total Environment 581(359-368.

4. Ashiq, A., M. Vithanage, B. Sarkar, M. Kumar, A. Bhatnagar, E. Khan, Y. Xi and Y. S. Ok (2021) Carbon-based adsorbents for fluoroquinolone removal from water and wastewater: A critical review. Environmental Research 197(111091. https://doi.org/10.1016/j.envres.2021.111091
5. Barko, J. W., D. G. Hardin and M. S. Matthews (1982) Growth and morphology of submersed freshwater macrophytes in relation to light and temperature. Canadian Journal of Botany 60(6):877-887. 10.1139/b82-113
6. Bergwerff, A. A. and P. Scherpenisse (2003) Determination of residues of malachite green in aquatic animals. Journal of chromatography. B, Analytical technologies in the biomedical and life sciences 788(2):351-359. 10.1016/s1570-0232(03)00042-4
7. Bhatt, S. and S. Chatterjee (2022) Fluoroquinolone antibiotics: Occurrence, mode of action, resistance, environmental detection, and remediation - A comprehensive review. Environmental pollution (Barking, Essex : 1987) 315(120440. 10.1016/j.envpol.2022.120440
8. Blake, S. L., S. H. Walker, D. C. Muddiman, D. Hinks and K. R. Beck (2011) Spectral Accuracy and Sulfur Counting Capabilities of the LTQ-FT-ICR and the LTQ-Orbitrap XL for Small Molecule Analysis. Journal of The American Society for Mass Spectrometry 22(12):2269-2275. 10.1007/s13361-011-0244-3
9. Boonsaner, M. and D. W. Hawker (2010) Accumulation of oxytetracycline and norfloxacin from saline soil by soybeans. Science of The Total Environment 408(7):1731-1737. https://doi.org/10.1016/j.scitotenv.2009.12.032
10. Crous, P. W. (2009) CBS laboratory manual series.
11. Čvančarová, M., M. Moeder, A. Filipová and T. Cajthaml (2015) Biotransformation of fluoroquinolone antibiotics by ligninolytic fungi – Metabolites, enzymes and residual antibacterial activity. Chemosphere 136(311-320. https://doi.org/10.1016/j.chemosphere.2014.12.012
12. Dai, Y., H. Tang, J. Chang, Z. Wu and W. Liang (2014) What's better, Ceratophyllum demersum L. or Myriophyllum verticillatum L., individual or combined? Ecological Engineering 70(397-401. https://doi.org/10.1016/j.ecoleng.2014.06.009
13. Gao, N., C.-X. Liu, Q.-M. Xu, J.-S. Cheng and Y.-J. Yuan (2018) Simultaneous removal of ciprofloxacin, norfloxacin, sulfamethoxazole by co-producing oxidative enzymes system of Phanerochaete chrysosporium and Pycnoporus sanguineus. Chemosphere 195(146-155. https://doi.org/10.1016/j.chemosphere.2017.12.062
14. Han, Q. F., S. Zhao, X. R. Zhang, X. L. Wang, C. Song and S. G. Wang (2020) Distribution, combined pollution and risk assessment of antibiotics in typical marine aquaculture farms surrounding the Yellow Sea, North China. Environ Int 138(105551. 10.1016/j.envint.2020.105551
15. Hoang, T. T., L. T. Tu, P. Le Nga and Q. P. Dao (2013) A preliminary study on the phytoremediation of antibiotic contaminated sediment. International journal of phytoremediation 15(1):65-76. 10.1080/15226514.2012.670316
16. Hoshino, Y., S. Fujii, H. Shinonaga, K. Arai, F. Saito, T. Fukai, H. Satoh, Y. Miyazaki and J. Ishikawa (2010) Monooxygenation of rifampicin catalyzed by the rox gene product of Nocardia farcinica:

structure elucidation, gene identification and role in drug resistance. The Journal of antibiotics 63(1):23-28. 10.1038/ja.2009.116

17. Huijbers, M. M. E., S. Montersino, A. H. Westphal, D. Tischler and W. J. H. van Berkel (2014) Flavin dependent monooxygenases. Archives of Biochemistry and Biophysics 544(2-17. https://doi.org/10.1016/j.abb.2013.12.005
18. Hwang, W. C., Q. Xu, B. Wu and A. Godzik (2018) Retraction: Crystal structure of a Baeyer-Villiger flavin-containing monooxygenase from Staphylococcus aureus MRSA strain MU50, William C. Hwang, Qingping Xu, Bainan Wu, Adam Godzik. Proteins 86(2):269. 10.1002/prot.24661
19. Ibrahim, S. R. M., S. G. A. Mohamed, A. E. Altyar and G. A. Mohamed (2021) Natural Products of the Fungal Genus Humicola: Diversity, Biological Activity, and Industrial Importance. Current microbiology 78(7):2488-2509. 10.1007/s00284-021-02533-6
20. Jensen, K. A., Jr., C. J. Houtman, Z. C. Ryan and K. E. Hammel (2001) Pathways for extracellular Fenton chemistry in the brown rot basidiomycete Gloeophyllum trabeum. Applied and environmental microbiology 67(6):2705-2711. 10.1128/aem.67.6.2705-2711.2001
21. Karl, W., J. Schneider and H. G. Wetzstein (2006) Outlines of an "exploding" network of metabolites generated from the fluoroquinolone enrofloxacin by the brown rot fungus Gloeophyllum striatum. Applied Microbiology and Biotechnology 71(1):101-113.
22. Karl, W., J. Schneider and H. G. Wetzstein (2006) Outlines of an "exploding" network of metabolites generated from the fluoroquinolone enrofloxacin by the brown rot fungus Gloeophyllum striatum. Appl Microbiol Biotechnol 71(1):101-113. 10.1007/s00253-005-0177-5
23. Larkin, M. A., G. Blackshields, N. P. Brown, R. Chenna, P. A. McGettigan, H. McWilliam, F. Valentin, I. M. Wallace, A. Wilm, R. Lopez, J. D. Thompson, T. J. Gibson and D. G. Higgins (2007) Clustal W and Clustal X version 2.0. Bioinformatics (Oxford, England) 23(21):2947-2948. 10.1093/bioinformatics/btm404
24. Li, W., Y. Shi, L. Gao, J. Liu and Y. Cai (2012) Occurrence of antibiotics in water, sediments, aquatic plants, and animals from Baiyangdian Lake in North China. Chemosphere 89(11):1307-1315. 10.1016/j.chemosphere.2012.05.079
25. Li, Y., J. Niu and W. Wang (2011) Photolysis of Enrofloxacin in aqueous systems under simulated sunlight irradiation: Kinetics, mechanism and toxicity of photolysis products. Chemosphere 85(5):892-897. https://doi.org/10.1016/j.chemosphere.2011.07.008
26. Lin, Z. Z., H. Y. Zhang, A. H. Peng, Y. D. Lin, L. Li and Z. Y. Huang (2016) Determination of malachite green in aquatic products based on magnetic molecularly imprinted polymers. Food chemistry 200(32-37. 10.1016/j.foodchem.2016.01.001
27. Liu, Z. and T. Wang (2012) Effects of pH on aquaculture. China Animal Husbandry and Veterinary Digest 12):99-99.
28. Ma, R., W. Fang, Z. Yang and K. Hu (2019) Liver proteome analysis of grass carp (Ctenopharyngodon idellus) following treatment with enrofloxacin. Fish physiology and biochemistry 45(6):1941-1952. 10.1007/s10695-019-00690-x

29. Minerdi, D., I. Zgrablic, S. Castrignanò, G. Catucci, C. Medana, M. E. Terlizzi, G. Gribaudo, G. Gilardi and S. J. Sadeghi (2016) Escherichia coli Overexpressing a Baeyer-Villiger Monooxygenase from Acinetobacter radioresistens Becomes Resistant to Imipenem. Antimicrobial agents and chemotherapy 60(1):64-74. 10.1128/aac.01088-15
30. Moreira, V. R., Y. A. R. Lebron, M. M. da Silva, L. V. de Souza Santos, R. S. Jacob, C. K. B. de Vasconcelos and M. M. Viana (2020) Graphene oxide in the remediation of norfloxacin from aqueous matrix: simultaneous adsorption and degradation process. Environmental Science and Pollution Research 27(27):34513-34528. 10.1007/s11356-020-09656-6
31. Pan, L.-j., J. Li, C.-x. Li, X.-d. Tang, G.-w. Yu and Y. Wang (2018) Study of ciprofloxacin biodegradation by a Thermus sp. isolated from pharmaceutical sludge. Journal of Hazardous Materials 343(59-67. https://doi.org/10.1016/j.jhazmat.2017.09.009
32. Parshikov, I. A. and J. B. Sutherland (2012) Microbial transformations of antimicrobial quinolones and related drugs. Journal of Industrial Microbiology & Biotechnology 39(12):1731-1740.
33. Pedersen, O., T. D. Colmer and K. Sand-Jensen (2013) Underwater photosynthesis of submerged plants - recent advances and methods. Frontiers in plant science 4(140. 10.3389/fpls.2013.00140
34. Prieto, A., M. Möder, R. Rodil, L. Adrian and E. Marco-Urrea (2011) Degradation of the antibiotics norfloxacin and ciprofloxacin by a white-rot fungus and identification of degradation products. Bioresource Technology 102(23):10987-10995. https://doi.org/10.1016/j.biortech.2011.08.055
35. Reis, R. A. G., H. Li, M. Johnson and P. Sobrado (2021) New frontiers in flavin-dependent monooxygenases. Arch Biochem Biophys 699(108765. 10.1016/j.abb.2021.108765
36. Riaz, L., T. Mahmood, A. Khalid, A. Rashid, M. B. Ahmed Siddique, A. Kamal and M. S. Coyne (2018) Fluoroquinolones (FQs) in the environment: A review on their abundance, sorption and toxicity in soil. Chemosphere 191(704-720. 10.1016/j.chemosphere.2017.10.092
37. Ricken, B. and B. A. Kolvenbach (2017) FMNH(2)-dependent monooxygenases initiate catabolism of sulfonamides in Microbacterium sp. strain BR1 subsisting on sulfonamide antibiotics. 7(1):15783. 10.1038/s41598-017-16132-8
38. RW, R. (1970) A mycological color chart. Commonwealth mycological institute and British mycological
39. Sangare, L., Y. Zhao, Y. M. E. Folly, J. Chang, J. Li, J. N. Selvaraj, F. Xing, L. Zhou, Y. Wang and Y. Liu (2014) Aflatoxin B1 Degradation by a Pseudomonas Strain. Toxins 6(10):3028-3040.
40. Santamaría, L. and W. van Vierssen (1997) Photosynthetic temperature responses of fresh- and brackish-water macrophytes: a review. Aquatic Botany 58(2):135-150. https://doi.org/10.1016/S0304-3770(97)00015-6
41. Santos, F., C. M. R. d. Almeida, I. Ribeiro, A. C. Ferreira and A. P. Mucha (2019) Removal of veterinary antibiotics in constructed wetland microcosms – Response of bacterial communities. Ecotoxicology and Environmental Safety 169(894-901. https://doi.org/10.1016/j.ecoenv.2018.11.078
42. Srivastava, S., R. Sinha and D. Roy (2004) Toxicological effects of malachite green. Aquatic toxicology (Amsterdam, Netherlands) 66(3):319-329. 10.1016/j.aquatox.2003.09.008

43. Tamura, K., D. Peterson, N. Peterson, G. Stecher, M. Nei and S. Kumar (2011) MEGA5: molecular evolutionary genetics analysis using maximum likelihood, evolutionary distance, and maximum parsimony methods. Molecular biology and evolution 28(10):2731-2739. 10.1093/molbev/msr121
44. Tripathi, P., P. Khare, D. Barnawal, K. Shanker, P. K. Srivastava, R. D. Tripathi and A. Kalra (2020) Bioremediation of arsenic by soil methylating fungi: Role of Humicola sp. strain 2WS1 in amelioration of arsenic phytotoxicity in Bacopa monnieri L. The Science of the total environment 716(136758. 10.1016/j.scitotenv.2020.136758
45. van Berkel, W. J. H., N. M. Kamerbeek and M. W. Fraaije (2006) Flavoprotein monooxygenases, a diverse class of oxidative biocatalysts. Journal of Biotechnology 124(4):670-689. https://doi.org/10.1016/j.jbiotec.2006.03.044
46. Van Caekenberghe, D. L. and S. R. Pattyn (1984) In vitro activity of ciprofloxacin compared with those of other new fluorinated piperazinyl-substituted quinoline derivatives. Antimicrobial agents and chemotherapy 25(4):518-521. 10.1128/aac.25.4.518
47. Van Doorslaer, X., J. Dewulf, H. Van Langenhove and K. Demeestere (2014) Fluoroquinolone antibiotics: an emerging class of environmental micropollutants. The Science of the total environment 500-501(250-269. 10.1016/j.scitotenv.2014.08.075
48. Volkers, G., G. J. Palm, M. S. Weiss, G. D. Wright and W. Hinrichs (2011) Structural basis for a new tetracycline resistance mechanism relying on the TetX monooxygenase. FEBS Letters 585(7):1061-1066. https://doi.org/10.1016/j.febslet.2011.03.012
49. Wang, X. W., J. Houbraken, J. Z. Groenewald, M. Meijer, B. Andersen, K. F. Nielsen, P. W. Crous and R. A. Samson (2016) Diversity and taxonomy of Chaetomium and chaetomium-like fungi from indoor environments. Stud Mycol 84(145-224. 10.1016/j.simyco.2016.11.005
50. Wang, X. W., F. Y. Yang, M. Meijer, B. Kraak, B. D. Sun, Y. L. Jiang, Y. M. Wu, F. Y. Bai, K. A. Seifert, P. W. Crous, R. A. Samson and J. Houbraken (2019) Redefining Humicola sensu stricto and related genera in the Chaetomiaceae. Studies in Mycology 93(65-153. https://doi.org/10.1016/j.simyco.2018.07.001
51. Wetzstein, Heinz-Georg, Schmeer and Norbert (1997) Degradation of the fluoroquinolone enrofloxacin by the brown rot fungus Gloeophyllum striatum. Applied & Environmental Microbiology
52. Wetzstein, H. G., J. Schneider and W. Karl (2006) Patterns of metabolites produced from the fluoroquinolone enrofloxacin by basidiomycetes indigenous to agricultural sites. Applied Microbiology and Biotechnology 71(1):90-100. 10.1007/s00253-005-0178-4
53. Wetzstein, H. G., M. Stadler, H. V. Tichy, A. Dalhoff and W. Karl (1999) Degradation of ciprofloxacin by basidiomycetes and identification of metabolites generated by the brown rot fungus Gloeophyllum striatum. Applied and environmental microbiology 65(4):1556-1563. 10.1128/aem.65.4.1556-1563.1999
54. Xu, G. and J. Wang (2014) Biodegradation of decabromodiphenyl ether (BDE-209) by white-rot fungus Phlebia lindtneri. Chemosphere 110(70-77. 10.1016/j.chemosphere.2014.03.052

55. Zhang, H. and C.-H. Huang (2007) Adsorption and oxidation of fluoroquinolone antibacterial agents and structurally related amines with goethite. Chemosphere 66(8):1502-1512. https://doi.org/10.1016/j.chemosphere.2006.08.024
56. Zhang, L., Y. Zhang and L. Liu (2019) Effect of submerged macrophytes Vallisneria spiralis L. on restoring the sediment contaminated by enrofloxacin in aquaculture ponds. Ecological Engineering 140(105596. https://doi.org/10.1016/j.ecoleng.2019.105596
57. Zhang, M., D. Fan, C. Su, L. Pan, Q. He, Z. Li and C. Liu (2023) Biotransformation of sulfamethoxazole by a novel strain, Nitratireductor sp. GZWM139: Characterized performance, metabolic mechanism and application potential. J Hazard Mater 441(129861. 10.1016/j.jhazmat.2022.129861

Figures

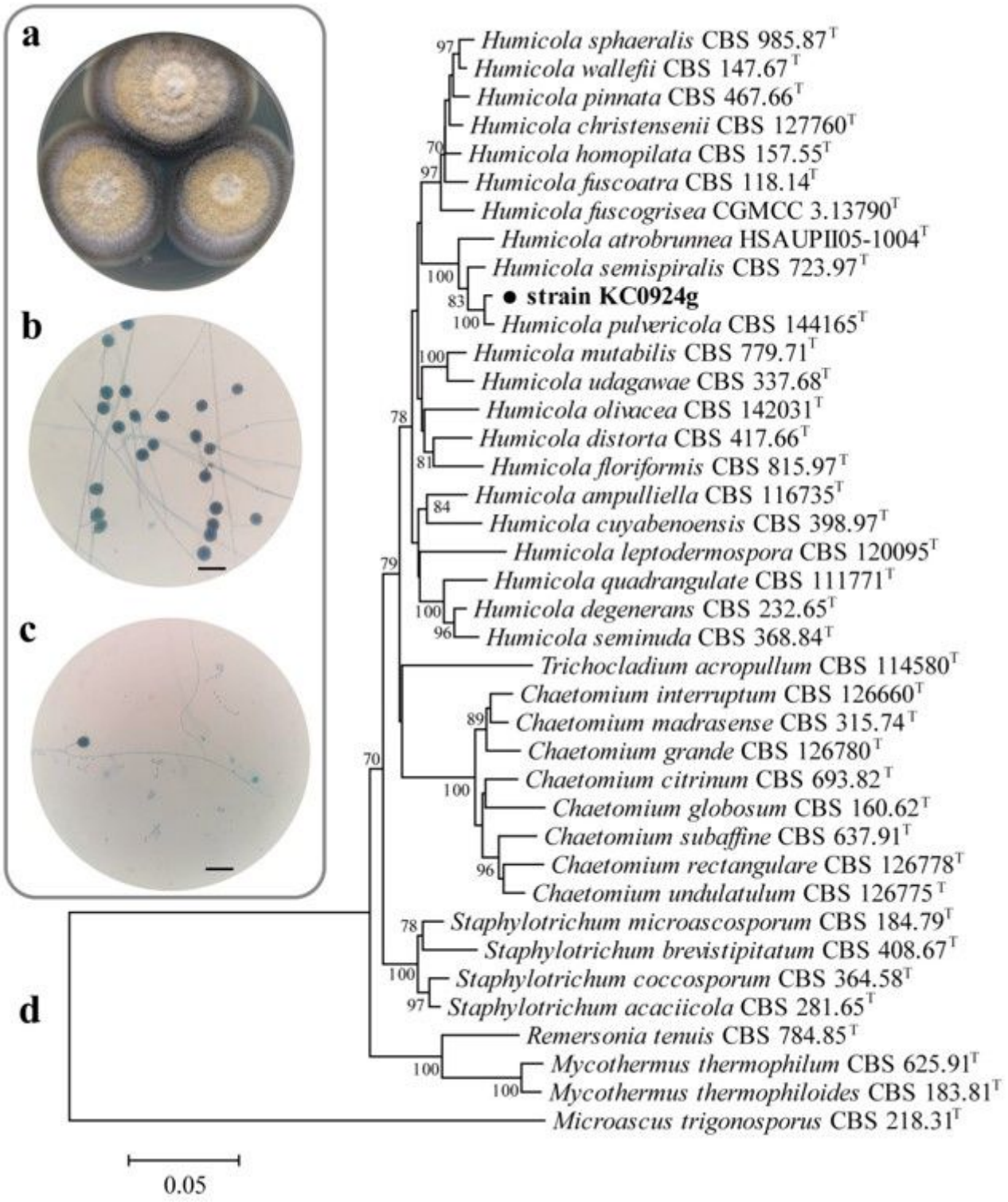

Figure 1

Photographs and phylogenetic dendrogram of strain KC0924g. **a**, Colony morphology on PDA medium; **b**, micromorphology of hyphae and thick-walled conidia; **c**, micromorphology of hyphae, thick-walled conidia and acremonium-like synanamorph; **d**, phylogenetic tree derived from ITS and LSU-*rpb2-tub2*sequences of strain KC0924g and related species.

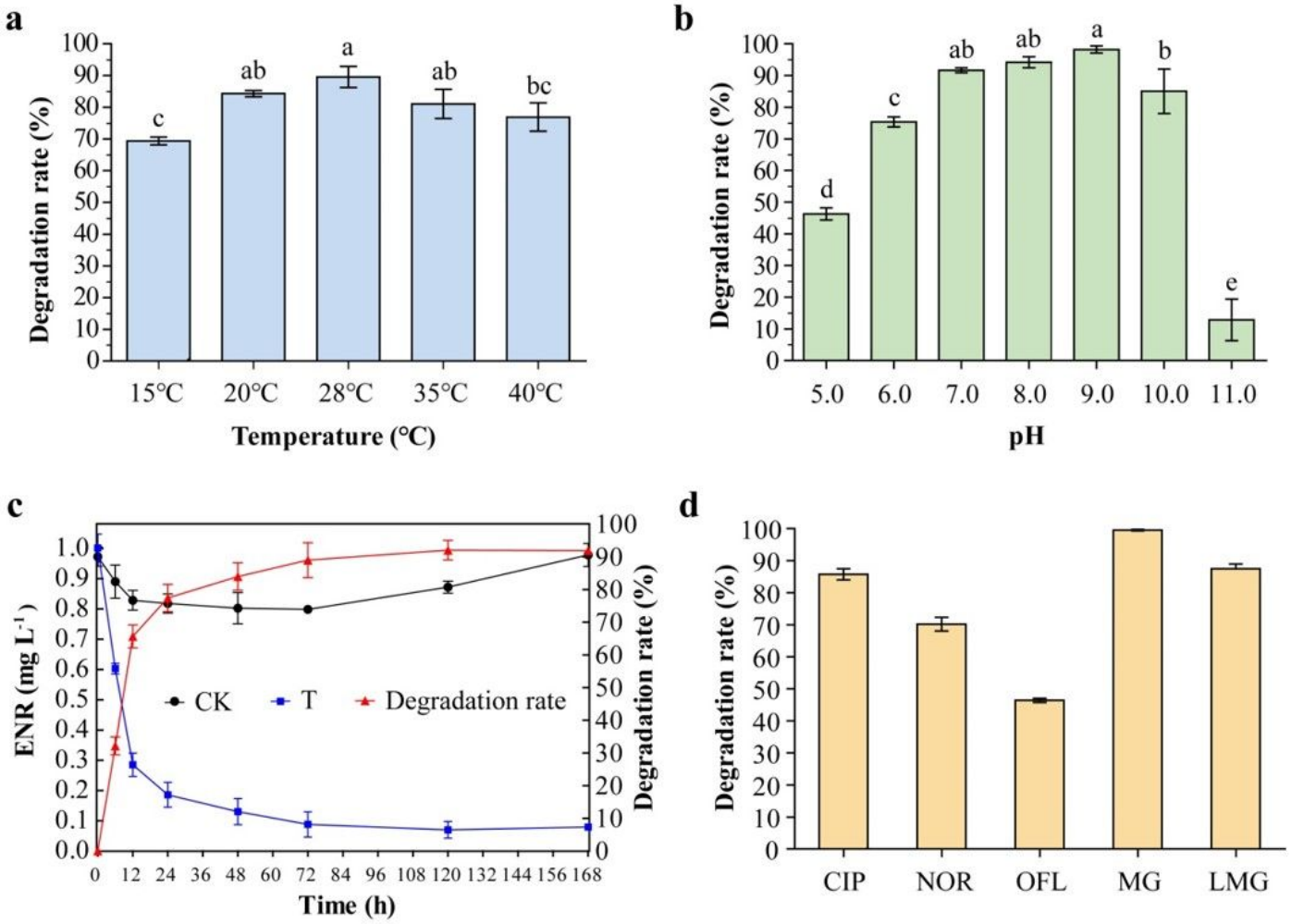

Figure 2

Degradation characteristics of strain KC0924g. **a**, Effect ofincubation temperature on the enrofloxacin degradation rate; **b**, effect of incubation pH on the enrofloxacin degradation rate; **c**, dynamic degradation curve of enrofloxacin; **d**, degradation rates of other fluoroquinolones, malachite green and leucomalachite green. Error bars represent the standard error of three replicates.

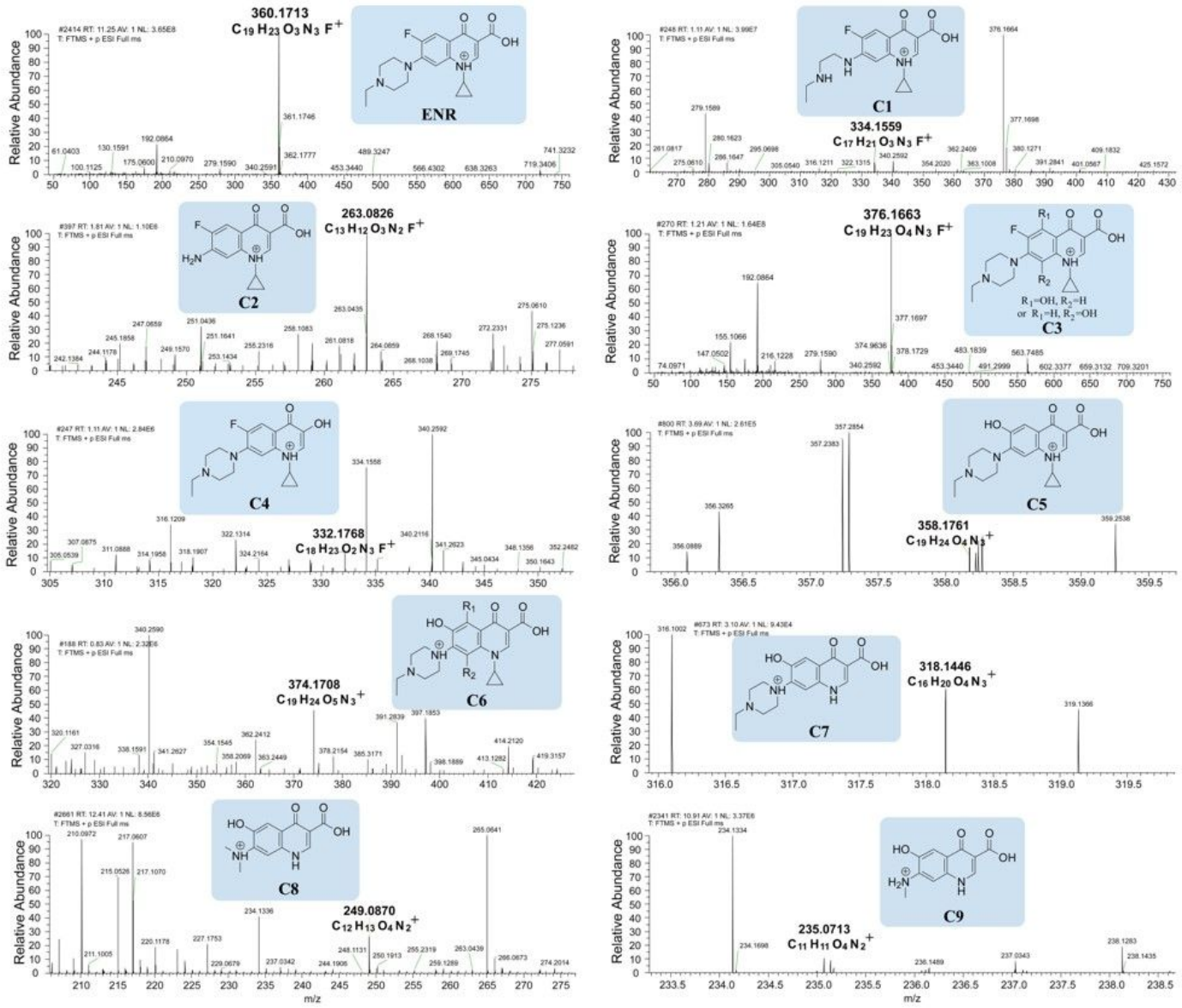

Figure 3

The main metabolites identified by UPLC–HRMS in cultures treated with strain KC0924g.

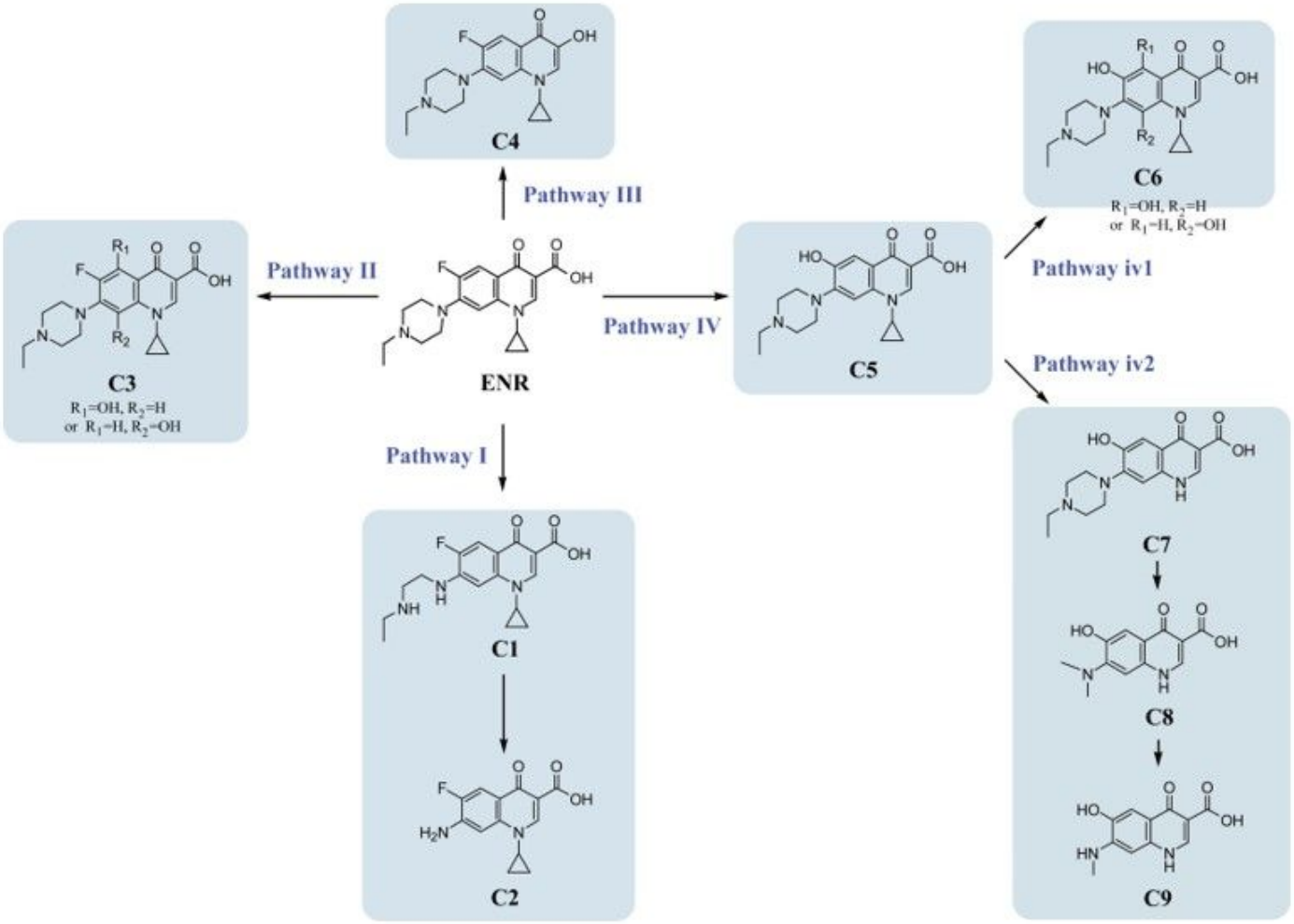

Figure 4

Proposed degradation pathway of enrofloxacin (ENR) by strain KC0924g. Pathway I, ENR degradation via decomposition of the piperazine moiety; Pathway II, ENR degradation via hydroxylation of the aromatic ring; Pathway III, ENR degradation via oxidative decarboxylation; Pathway IV, ENR degradation via oxidative defluorination.

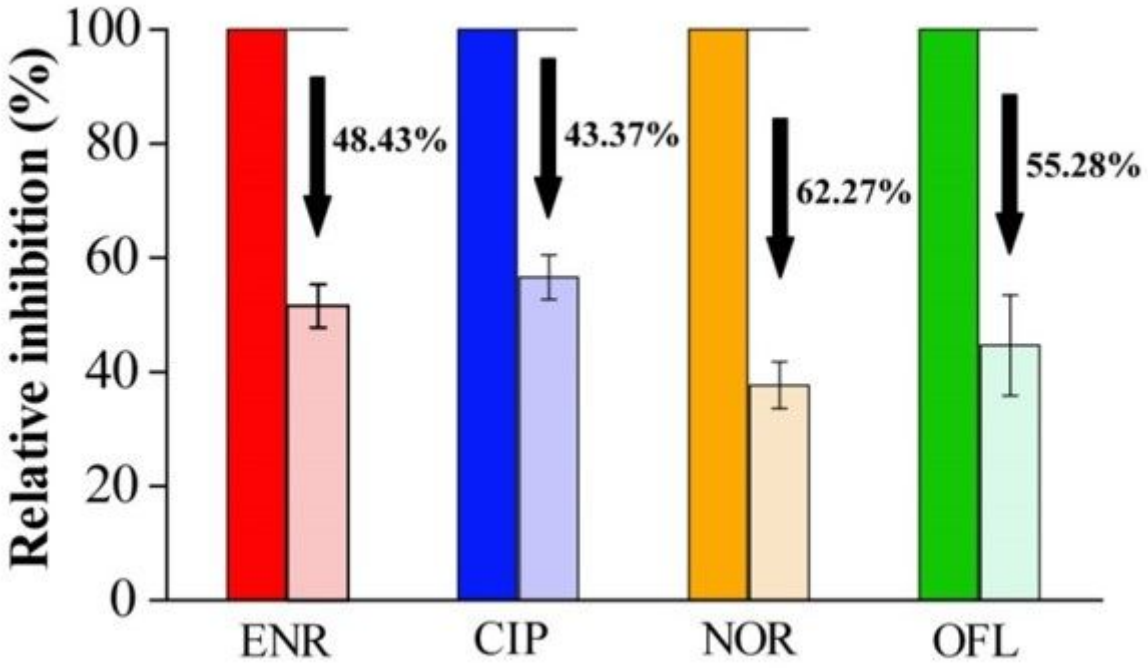

Figure 5

Relative changes in inhibition of four fluoroquinolones (FQs) in MM medium after 72 hours of incubation with strain KC0924g. Bars filled with a darker color represent the initial antibacterial activity of the four FQs and are defined as 100%. Bars filled with a lighter color indicate the relative inhibition of the four FQs in MM medium after 72 hours of incubation with strain KC0924g.

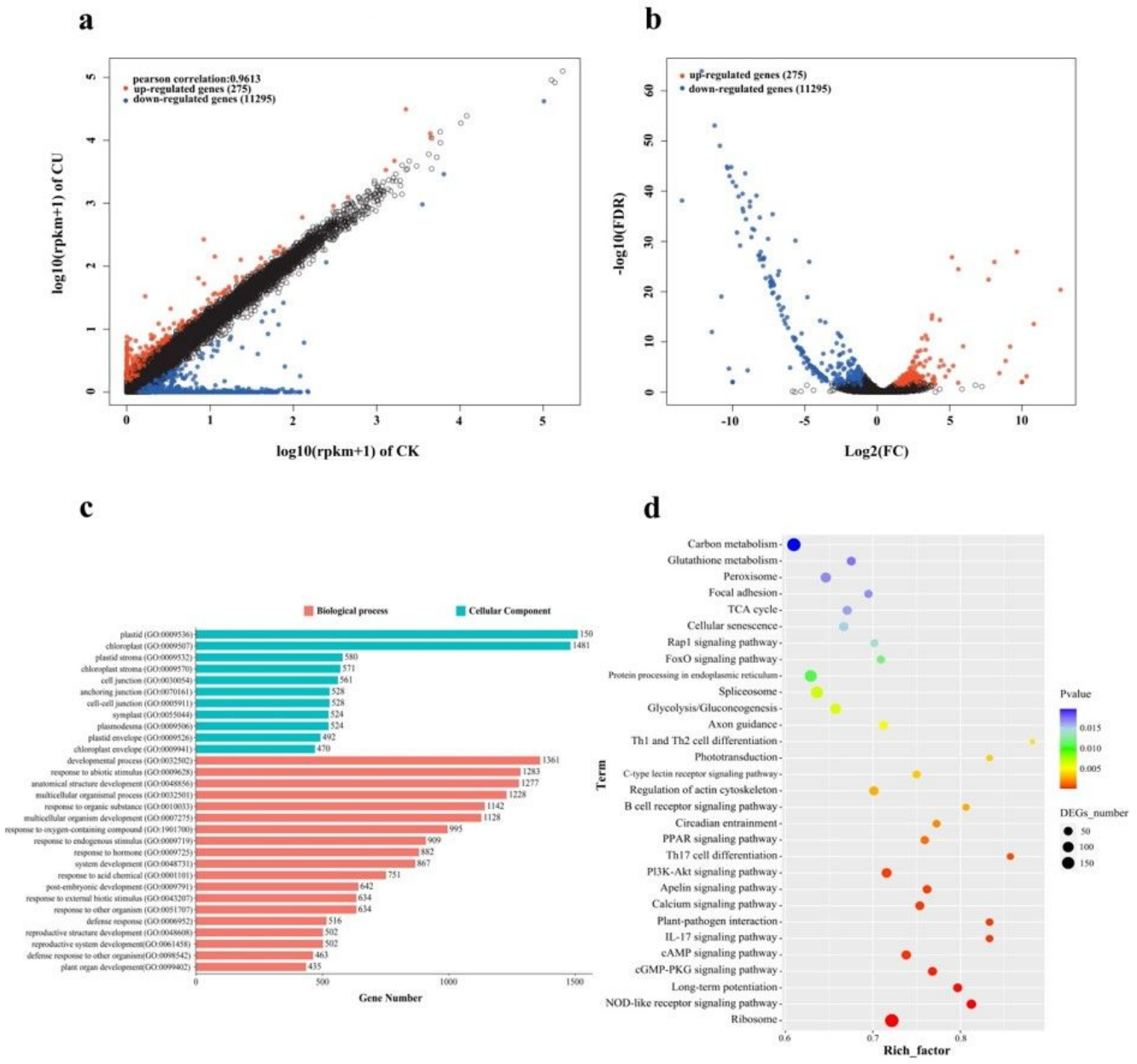

Figure 6

Scatter plot (a), Volcano plot (b), GO enrichment analysis (c) and KEGG enrichment analysis (d) of differentially expressed genes between the CK and CU groups.

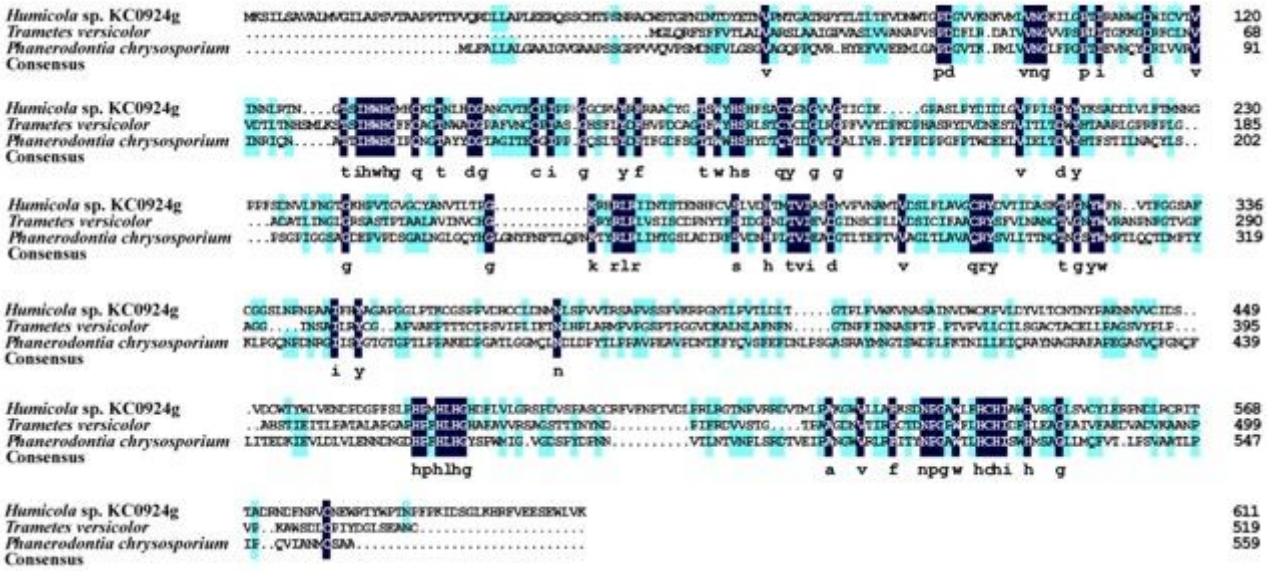

Figure 7

BLAST analysis of the amino acid sequences of laccase from three fungi.

Supplementary Files

This is a list of supplementary files associated with this preprint. Click to download.

- Supplementarymaterials.docx